J Biomol NMR (2008) 40:165–174
DOI 10.1007/s10858-007-9216-0

ARTICLE

Dynamic inter-subunit interactions in thermophilic F_1-ATPase subcomplexes studied by cross-correlated relaxation-enhanced polarization transfer NMR

Masumi Kobayashi · Hiromasa Yagi · Toshio Yamazaki · Masasuke Yoshida · Hideo Akutsu

Received: 31 August 2007 / Accepted: 3 December 2007 / Published online: 5 January 2008

Abstract F_1-ATPase is a unique enzyme in terms of its rotational catalytic activity. The smallest unit showing this property is the $\alpha_3\beta_3\gamma$ complex (351 kDa). For investigation of such a huge system by means of solution NMR, we have explored a suitable NMR method using F_1-ATPase subcomplexes from a thermophilic Bacillus PS3 including an $\alpha_3\beta_3$ hexamer (319 kDa). Pulse sequences for large molecules, effects of deuteration and simplification of the spectra were examined in this work. Since the β subunit includes the catalytic site, this was the target of the analysis in this work. The combination of [^{15}N,^{1}H]-CRINEPT-HMQC-[^{1}H]-TROSY, deuteration of both α and β subunits, and segmental isotope-labeling was found essential to analyze such a huge and complex molecular system. Utilizing this method, subcomplexes composed of α and β subunits were investigated in terms of inter-subunit interactions. It turned out that there is equilibrium among monomers, heterodimers and the $\alpha_3\beta_3$ hexamers in solution. The rate of exchange between the dimer and hexamer is in the slow regime on the NMR time scale. In chemical shift perturbation experiments, the N-terminal domain was found to be involved in strong inter-subunit interactions. In contrast, the C-terminal domain was found to be mobile even in the hexamer.

Keywords CRINEPT · CRIPT · H^+-ATPsynthase · Large molecule · Segmental isotope-labeling · TROSY

Abbreviations

TF_1-ATPase	F_1-ATPase from thermophilic Bacillus PS3
TROSY	Transverse relaxation-optimized spectroscopy
CRIPT	Cross-correlated relaxation-induced polarization transfer
CRINEPT	Cross-correlated relaxation-enhanced polarization transfer
HMQC	Heteronuclear multiple quantum correlation
INEPT	Insensitive nuclei enhanced by polarization transfer

Introduction

H^+-ATP synthase is a huge multisubunit enzyme that consists of membrane-embedded F_0 ($ab_2c_{10\text{-}14}$) and soluble F_1 ($\alpha_3\beta_3\gamma\delta\varepsilon$), and synthesizes/hydrolyzes ATP conjugating with H^+-translocation (Boyer 1997; Capaldi and Aggeler 2002). The crystal structure of mitochondrial F_1 revealed that three α and β subunits form a complex interacting alternatively in a ring formation with the γ subunit penetrating the central hole (Abrahams et al. 1994). It was also shown that the catalytic site was located in the β subunit at the α/β interface. Subsequently, the rotation of $\alpha_3\beta_3\gamma$ from thermophilic Bacillus PS3 F_1 (TF_1) was proved to be

Electronic supplementary material The online version of this article (doi:10.1007/s10858-007-9216-0) contains supplementary material, which is available to authorized users.

M. Kobayashi · H. Yagi · H. Akutsu (✉)
Institute for Protein Research, Osaka University,
3-2 Yamadaoka, Suita, Osaka 565-0871, Japan
e-mail: akutsu@protein.osaka-u.ac.jp

T. Yamazaki
RIKEN G.S.C, 214 Maeda-cho, Totsuka-ku, Yokohama,
Kanagawa 244-0804, Japan

M. Yoshida
Chemical Resources Laboratory, Tokyo Institute of Technology,
2-12-1 Ookayama, Meguro-ku, Tokyo 152-8550, Japan

coupled with ATP hydrolysis (Noji et al. 1997). These observations support the binding-change mechanism proposed by Boyer (1993). The details of the rotational catalytic mechanism and the F_1 structure during rotation have not yet been clarified because the crystal structures (Abrahams et al. 1994) do not directly show the structures in the catalytic reaction. In particular, the structure and dynamics of the β subunit, which plays a crucial role in the rotation and catalytic reaction, should be examined in a more natural situation. Nuclear Magnetic Resonance (NMR) spectroscopy is one of the most suitable methods for this purpose. We have already reported that the conformational change of the β subunit monomer induced by nucleotide binding is one of its intrinsic property and that this is actually one of the driving forces of the rotation (Yagi et al. 1999, 2004; Tozawa et al. 2001). For comprehensive elucidation of the rotational catalytic mechanism, however, the whole F_1 complex should be analyzed by means of NMR.

A serious problem for solution NMR is the size limit. To overcome this, Wüthrich and his colleagues developed NMR pulse sequences for macromolecular systems, namely, transverse relaxation-optimized spectroscopy (TROSY) (Fernández and Wider 2003), cross relaxation-induced polarization transfer (CRIPT), and cross-correlated relaxation-enhanced polarization transfer (CRINEPT) (Brüschweiler and Ernst 1992; Riek et al. 1999, 2002), and then succeeded in measuring an isotope-labeled 10 kDa subunit in a 900 kDa GroEL–GroES complex by means of CRIPT-TROSY (Fiaux et al. 2002). Kay and his colleagues have also been developing new methods for large molecules (Tugarinov et al. 2004; Mittermaier and Kay 2006; Yang and Kay 1999). Recently, they reported structural analysis of the 20 S proteosome (670 kDa) using methyl protons in the fully deuterated protein (Sprangers and Kay 2007). We would like to focus on the backbone conformation in this work because of the drastic conformational change in the β subunit of F_1 on nucleotide binding. Even the β subunit itself was shown to be difficult for NMR analysis because of its large molecular mass (52 kDa) without segmental isotope-labeling (Yagi et al. 2004). Since the molecular mass of the $\alpha_3\beta_3\gamma$ complex (351 kDa) is much larger than that of the β subunit, a method for this type of large molecule was developed in this work.

The F_1-ATPase from thermophilic Bacillus PS3 (TF_1) was used for this purpose because of its thermal stability (Yoshida et al. 1975), and the high efficiency of reconstitution from individual purified subunit (Yoshida et al. 1977). The TF_1 $\alpha_3\beta_3$ hexamer could be separated by gel filtration column chromatography (Kagawa et al. 1989; Miwa and Yoshida 1989; Saika and Yoshida 1995) and successfully crystallized for structure determination (Shirakihara et al. 1997). In the crystal structure, all three β subunits take on the open forms, showing a three-fold symmetry. This high symmetry is an advantage for high resolution analysis in solution. Not only the $\alpha_3\beta_3\gamma$ complex but also the $\alpha\beta$ heterodimer (110 kDa) and $\alpha_3\beta_3$ hexamer have been reported to show ATPase activity (Miwa and Yoshida 1989). On the other hand, $\alpha_3\beta_3$ has been shown to dissociate into heterodimers in the presence of nucleotides (Kagawa et al. 1989), while $\alpha_3\beta_3\gamma$ does not under the same conditions. This indicates that the hexamer structure is not stable enough for the enzyme reaction. Therefore, the dynamic properties of the $\alpha\beta$ heterodimer and $\alpha_3\beta_3$ hexamer were investigated in this work to understand the stability of the hexamer structure.

To obtain high resolution spectra of the $\alpha_3\beta_3$ hexamer, the combination of [^{15}N,^{1}H]-CRINEPT-HMQC-[^{1}H]-TROSY, deuteration of both α and β subunits, and segmental isotope-labeling was found to be essential in this work. The application of this method to the subcomplexes showed equilibrium among monomers, heterodimers and hexamers, and also the dynamic property of the β subunit in the subcomplexes.

Materials and methods

Purification of α and β subunits

The F_1 α gene from thermophilic Bacillus PS3 (Ohta et al. 1988) was inserted into plasmid pET32a (Novagen Inc., Madison, WI). *Escherichia coli* BL21(DE3) (Novagen Inc.) was used as a host strain. The transformed cells were grown in LB medium. Cells were grown for 5 h after induction with 1 mM isopropyl-β-D-thiogalactopyranoside (IPTG), then harvested and disrupted. The supernatant was applied to a Toyopearl DEAE-650M column (Tosoh Co., Tokyo, Japan) equilibrated with buffer A [20 mM Tris–HCl, pH 8.0, 1 mM ethylenediamine tetraacetic acid (EDTA), and 1 mM dithiothreitol (DTT)], followed by elution with a linear gradient of 0–500 mM NaCl. Ammonium sulfate was added to the α subunit fraction up to 20% saturation for purification with a HiTrap^{TM} Phenyl HP column (GE Healthcare UK Ltd, Buckinghamshire, England). The column was eluted with a linear gradient of 20–0% saturated ammonium sulfate. Finally, the α fraction obtained was applied to a Superdex200 column (GE Healthcare UK Ltd) with buffer A. The purified α subunit was stored as an 80% saturated ammonium sulfate suspension at 4 °C. To obtain the deuterated α subunit, 95% or 80% $^{2}H_2O$ was used for the medium.

The TF_1 β subunit was obtained by substitution of the α gene with the β gene (Ohta et al. 1988) using the procedure mentioned above. For ^{15}N-labeling and high deuteration,

the transformed cells were cultured in M9 medium including d_6-glucose and $^{15}NH_4Cl$. Although the fully deuterated β was purified in H_2O buffers, around 10 N^2H groups remained in the NMR sample. Segmentally-labeled ones were prepared as in the previous study (Yagi et al. 2004). Since unfolding and refolding of the ligated β subunit in a H_2O buffer was included in the preparation procedure, protons replaced all exchangeable deuterons. The N-terminal (residues 1–124) and C-terminal (residues 391–473) domains were labeled independently. The former can be used for monitoring interactions with the neighboring α subunit in oligomers, and the latter would be a good probe for a conformational change and interactions with the γ subunit.

The deuterated α and β subunits were examined as to their deuteration ratio by means of MALDI-TOF-MS with an Autoflex (Bruker Daltonics K.K., Tsukuba, Japan). The actually deuterated fraction was 50–80% for both subunits.

NMR measurements

The α and β subunits precipitated on 80% ammonium sulfate saturation were dissolved in a complex reconstitution buffer (50 mM Tris-HCl, pH 8.0, 100 mM Na_2SO_4, and 0.1 mM $MgSO_4$) (Miwa and Yoshida 1989; Kagawa et al. 1989; Saika and Yoshida 1995). The β subunit monomer was dissolved at 0.3 mM in 450 µL including 10% ^2H_2O. For titration with the α subunit, mixtures of α and β subunits (α/β mixtures) were adjusted to α/β ratios of 0.5, 1 and 2, and the concentration of β subunit in each sample was kept constant at 0.13 mM in 330–350 µL including 10% ^2H_2O.

NMR spectra were recorded on a Bruker DRX-800 NMR spectrometer (Karlsruhe, Germany) equipped with a cryoprobe™ at 40 °C. All kinds of spectra were recorded with data size of 160 (^{15}N) × 2048 (^1H) complex points for monomer, and 128 (^{15}N) × 2048 (^1H) complex points for α subunit titration. The [^{15}N,^1H]-heteronuclear single quantum correlation (HSQC)-TROSY spectra (Yang and Kay 1999) were recorded with spectral widths of 3086 Hz (F_1) and 12820 Hz (F_2). The [^{15}N,^1H]-CRINEPT-heteronuclear multiquantum correlation (HMQC)-[^1H]-TROSY and [^{15}N,^1H]-CRIPT-TROSY spectra (Riek et al. 1999) were obtained with spectral widths of 2,840 Hz (^{15}N) × 16,025 Hz (^1H). CRINEPT and CRIPT transfer times were 3, and 4.4 ms, respectively. The accumulation number for each FID and a typical measurement time for CRINEPT and CRIPT were less than 160 and about 14 h for α/β mixtures, respectively. All NMR data were processed using NMRPipe and NMRDraw (Delaglio et al. 1995), and analyzed with Sparky (Goddard and Kneller 2006).

Results

Development of an NMR method for analysis of F_1 subcomplexes

As the first step to investigate the structure and function of $\alpha_3\beta_3\gamma$ by NMR, a suitable NMR method was explored using F_1 subcomplexes composed of α and β subunits. Since one of them, the $\alpha_3\beta_3$ hexamer, has a molecular mass of 319 kDa, the method developed in this work can be applied to the $\alpha_3\beta_3\gamma$ complex (351 kDa). For this purpose, we examined the three kinds of pulse sequences developed for the analysis of large molecules (Fernández and Wider 2003; Brüschweiler and Ernst 1992; Riek et al. 1999, 2002; Fiaux et al. 2002). [^{15}N,^1H]-TROSY (TROSY), [^{15}N,^1H]-CRINEPT-HMQC-[^1H]-TROSY (CRINEPT) and [^{15}N,^1H]-CRIPT-TROSY (CRIPT) spectra of the [U-^{15}N, ^2H]-labeled β subunit were recorded in the absence and presence of the α subunit (at $\alpha/\beta = 1$ and 2). The spectra for TROSY and CRINEPT are presented in Fig. 1. For the β monomer, the TROSY spectrum (Fig. 1a) is clearer than CRINEPT one (Fig. 1d). The CRIPT spectrum exhibited less signals because of cancellation due to overlapping of positive and negative signals (spectrum not shown). The CRINEPT spectrum in Fig. 1d showed most signals from the 473 residues, but it was more complicated than the TROSY one because of splitting into doublets. The monomer is too small for CRIPT and CRINEPT pulse sequences to cancel the fast relaxation components. The number of TROSY signals decreased with an increase in the α/β ratio (Fig. 1b and c). In contrast, CRINEPT provided enough signals in spite of line-broadening (Fig. 1e and f). The α and β subunits form larger oligomers under these conditions (Miwa and Yoshida 1989; Kagawa et al. 1989). Their molecular weights might be too large for TROSY to provide a spectrum of good quality. On CRIPT, the in-phase and anti-phase components of neighboring signals canceled each other out, presumably because of the presence of flexible regions. Thus, CRINEPT turned out to be appropriate for the analysis of TF_1 subcomplexes.

As the next step, the effect of deuteration of the α and/or β subunits was examined at $\alpha/\beta = 1$ by means of CRINEPT-HMQC-TROSY. Figure 2a shows a spectrum of an α/^{15}N-β subunit mixture without deuteration (^1H-α/^1H-β). Fig. 2b and c are those with only β deuterated (^1H-α/^2H-β) and both deuterated (^2H-α/^2H-β), respectively. The signals were getting sharper and sharper, and their resolution was more and more improved, as can be seen in the figures. Therefore, all subunits in the subcomplexes should be deuterated.

Even in Fig. 2c, the signals are too congested for analysis. To reduce the number of signals, segmental ^{15}N-labeling of the β subunit with intein (Yagi et al. 2004)

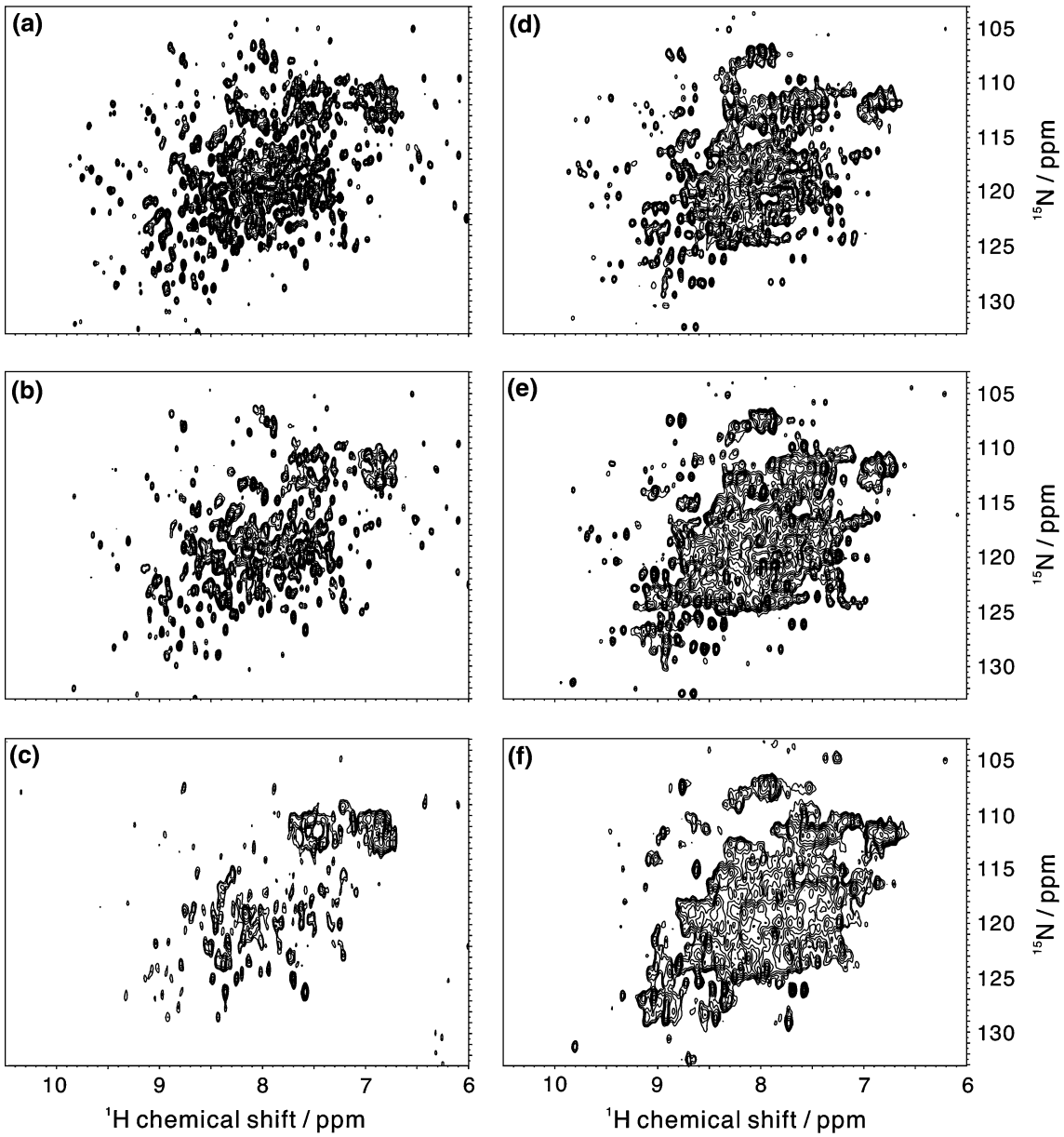

Fig. 1 [^{1}H,^{15}N]-HSQC-TROSY (**a**, **b** and **c**) and [^{1}H,^{15}N]-CRINEPT-HMQC-[^{1}H]-TROSY (**d**, **e** and **f**) spectra of the uniformly ^{15}N-labeled β subunit and the α/β mixtures at 313 K. The top, middle and bottom panels are for $\alpha/\beta = 0$ (monomer), $\alpha/\beta = 1$ and 2, respectively. The α and β subunits are 50 and 60% deuterated, respectively

was carried out. Two kinds of samples were obtained. One was labeled in the region of residues 1–124 (β^{*}(1–124)) and the other in that of residues 391–473 (β^{*}(391–473)). Here, β^{*} stands for the segmentally ^{15}N-labeled β subunit. The former and latter are labeled in the N- and C-terminal domains, respectively. CRINEPT spectra of α/β^{*}(1–124) and α/β^{*}(391–473) mixtures are presented in Fig. 3. Their resolutions were much improved in comparison with Fig. 2c and Fig. 1f. This can be used for chemical shift analysis. Although five extra residues were inserted into the ligation point through the intein reaction, the segmentally labeled signals were identical to those of the uniformly labeled samples (Yagi et al. 2004).

Consequently, we decided to utilize CRINEPT, deuteration of both α and β subunits and segmental-labeling of the β subunit for the analysis of F_1 subcomplexes.

Analysis of α/β^{*} mixtures

At first we isolated the $\alpha_3\beta_3$ hexamer on a gel filtration column of Superdex200 (GE Helthcare Bio-Sciences

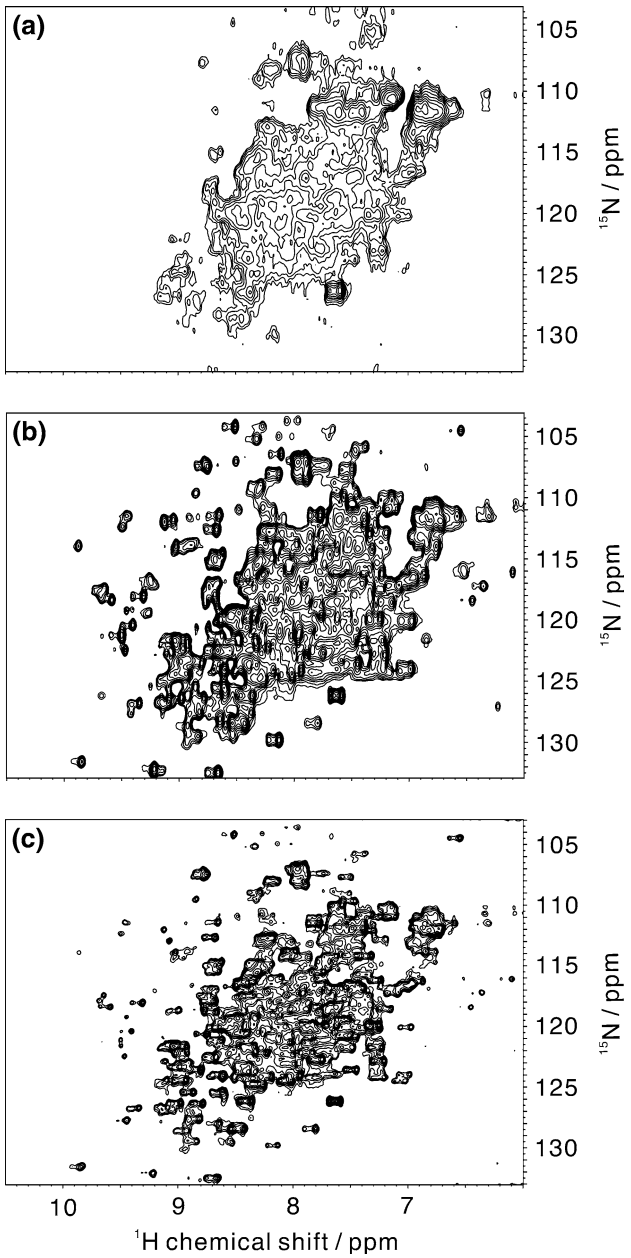

Fig. 2 Effect of deuteration on the CRINEPT-HMQC-TROSY spectrum of the uniformly ^{15}N-labeled β subunit in the α/β (=1) mixture. (**a**) Non-deuterated (^{1}H-α/^{1}H-β). (**b**) The β subunit is 80%-deuterated (^{1}H-α/^{2}H-β). (**c**) Both are 80% deuterated (^{2}H-α/^{2}H-β)

Corp.), according to the reported method (Miwa and Yoshida 1989; Kagawa et al. 1989). However, the obtained CRINEPT spectrum was too complicated. It included two different types of signals, broad singlets and sharp doublets. This was not due to the degradation of proteins as judged on SDS-PAGE. This suggested that smaller molecular species are present in the sample solution, in other words, the hexamers dissociate to some extent. Therefore, we tried to identify the origin of the signals by changing the amount of the α subunit. We prepared sample solutions containing two subunits at $\alpha/\beta^{*} = 0$, 0.5, 1 and 2, using two kinds of segmentally labeled samples, namely, β^{*}(1–124) and β^{*}(391–473). The assignments were made with reference to the β monomer chemical shifts that had already been reported (Yagi et al. 2004; BMRB No. 5886).

Typical behavior of the CRINEPT signals for each labeled region on changing of the α/β^{*} ratio is presented in Fig. 4. Signals in the N-terminal region revealed larger chemical shift changes than those in the C-terminal region. For example, Gly93 shows a doublet at 9.52 ppm, which moved to 9.49 ppm in the ^{1}H dimension with an increase in the α subunit concentration from $\alpha/\beta = 0$ to 1 (Fig. 4a, in red). Concomitantly, a broad and weak singlet appeared at 9.41 ppm. At $\alpha/\beta = 2$ the broader singlet became more intense without a shift, and the doublet got weaker at 9.48 ppm (green). Since the chemical shift of the doublet at $\alpha/\beta = 0.5$ was 9.49 ppm, it does not move as well from $\alpha/\beta^{*} = 0.5$ to 2. In the CRINEPT spectrum, a doublet appears when the pair of spins is involved in a rapid motion and only a singlet is observed when the motion is suppressed. It is known that TF_1 has mainly two subcomplexes, α/β heterodimer and $\alpha_3\beta_3$ hexamer (Saika and Yoshida 1995). In view of their molecular masses, the doublet and singlet in Fig. 4a can be ascribed to the heterodimer and hexamer, respectively.

From $\alpha/\beta = 0$ to 1, most signals in Fig. 3a and c were doublets. The intensity ratio obtained from the signal of Gly93 in Fig. 4a was 5.1:1.0. The amount of the hexamer would be underestimated because of the faster relaxation. Nevertheless, this result seems to conflict with the fact that the hexamer could be crystallized at $\alpha/\beta = 1$ (Shirakihara et al. 1997). However, the crystallization would depend on the protein concentration and solvent condition. At $\alpha/\beta = 2$, the aspect of the spectrum changed. The intensity ratio of the dimer to hexamer became 1.0:4.7 for the signal of Gly93 (Fig. 4a: green), showing that the hexamer is dominant at $\alpha/\beta = 2$. The line-widths on the ^{1}H axis were 35 and 87 Hz for the dimer and hexamer signals, respectively.

Now we can conclude that there is equilibrium as follows.

3 α monomer + 3 β monomer $\leftrightarrows$ 3 heterodimer $\leftrightarrows$ $\alpha_3\beta_3$ hexamer

The amounts of the heterodimer and hexamer were changed by titration of α subunit in this work. The rate of exchange between the dimer and $\alpha_3\beta_3$ hexamer is in the slow regime on the NMR time scale. This seems also the case with the heterodimer and monomers. However, the situation for the dimer is not straightforward, because there is no detectable monomer signals at $\alpha/\beta = 0.5$ (spectrum not shown). Furthermore, there are two possible configurations for the heterodimer, namely, one with the α subunit on the catalytic side of the β subunit ($\beta\alpha$ type), and the

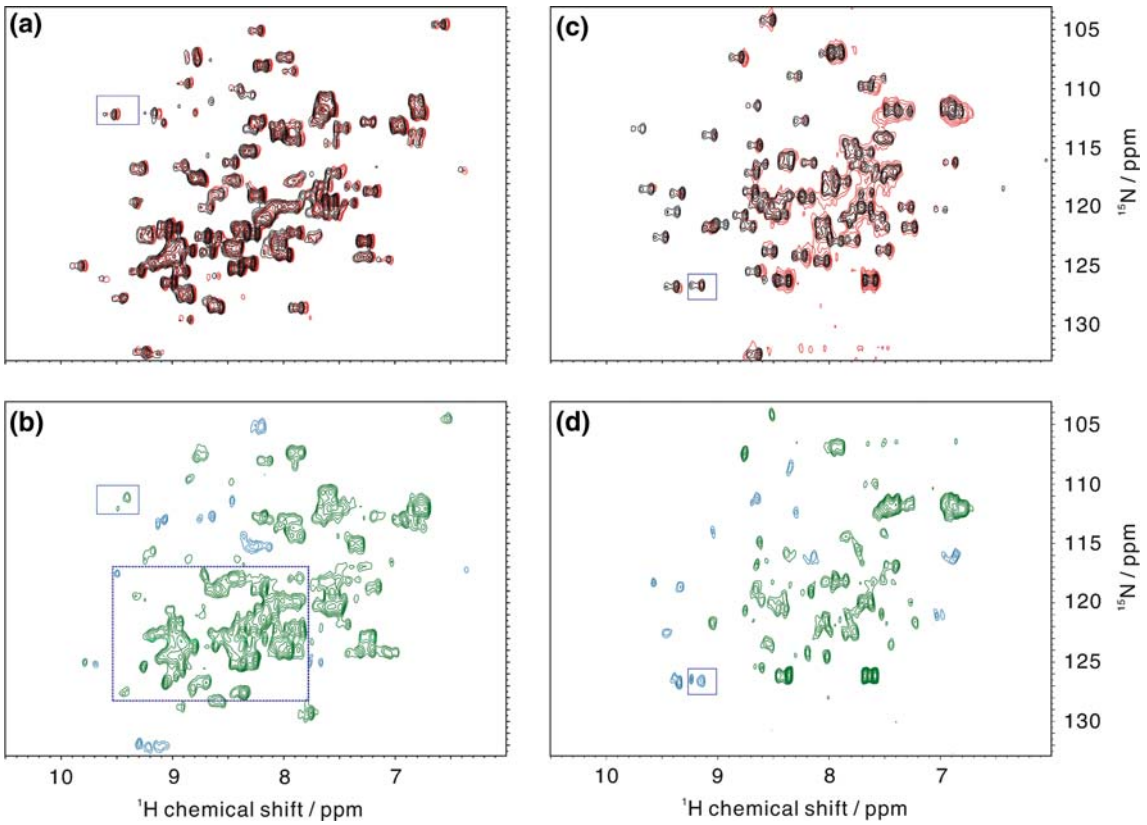

Fig. 3 CRINEPT-HMQC-TROSY spectra of the β subunit segmentally ^{15}N-labeled in the N- (1–124 residues) and C- (391–473 residues) terminal domains. The former is on the left (**a** and **b**), and the latter on the right (**c** and **d**). (**a**) and (**c**), the spectra at $\alpha/\beta^* = 0$ and 1 are shown in black and red, respectively. (**b**) and (**d**), at $\alpha/\beta^* = 2$. Signals obtained in a lower threshold are shown in blue. An expanded spectrum of the dotted frame is given in the supplementary Fig. S1. β^* stands for the segmentally ^{15}N-labeled β subunit. The α and β subunits are 50 and 60% deuterated, respectively

other with it on the opposite, non-catalytic side ($\alpha\beta$ type). A possible explanation for this observation is that either $\beta\alpha$ or $\alpha\beta$ is involved in the slow exchange and the other is in the intermediate-rate exchange with the monomer. The latter would cause a broadening of the monomer signal. If this is the case, the stability of the dimer is different for $\beta\alpha$ and $\alpha\beta$. Although there is no biochemical evidence so far, we cannot eliminate a possibility of trimer ($\beta\alpha\beta$) formation.

As shown in Fig. 4b, some signals for the C-terminal domain were remained as doublets for $\alpha/\beta = 0$ to 2. The signal in Fig. 4b is Phe409, which is next to a loop region of the C-terminal domain. Its apparent τ_c should be much smaller even in the hexamer, suggesting that the loop region is flexible (Riek et al. 1999). Regarding the linewidths of Phe409 on the ^{1}H axis, black, red and green, denote 36, 48, and 60 Hz, respectively (Fig. 4b).

Since the major species at $\alpha/\beta = 1$ and 2 are the heterodimer and hexamer signals, respectively, these spectra could be used to determine their chemical shifts. Minor peaks were not always observed, which made the spectra simpler than expected. Although some areas in Fig. 3b look congested, most signals could be identified with the better appodization and expansion of the spectrum as shown in supplementary Fig. S1 (available on line). The signals of the β monomer had already been assigned (Yagi et al. 2004). The assignment was transferred to the dimer signals on the basis of the proximity as far as the chemical shift change is small as shown in the top panel of Fig. S1. Although 115 and 80 cross peaks are expected for the β^*(1–124) and β^*(391–473) monomers, respectively, because of proline residues, 105 and 74 signals could be identified on their 2D CRINEPT spectra. At $\alpha/\beta = 1$, 93 and 74 cross peaks could be assigned for the former and the latter, respectively. In the case of the hexamer, the close proximity to the dimer signals was used for the assignment as far as the chemical shift change is small as shown in the bottom panel of Fig. S1. The assigned cross peaks for β^*(1–124) and β^*(391–473) were 93 and 69, respectively. Since the signals for β^*(1–124) were partly congested, we performed ^{15}N-Thr labeling, which led to the specific labeling of 7 Thr, 2 Ser and 10 Gly because of metabolic conversion. The spectra were used for the assignment of the congested signals as shown in Fig. S2 for $\alpha/\beta = 0$ and 2 (available on line).

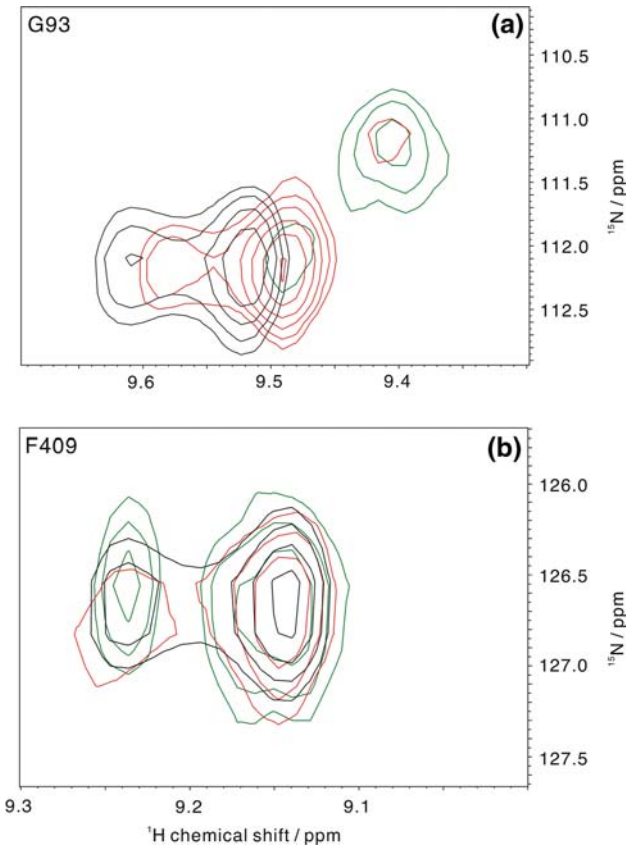

Fig. 4 Expansion of the square boxes in Fig. 3. Black, red and green lines stand for the signals at $\alpha/\beta^{*} = 0{,}1$ and 2, respectively. (**a**), Gly93; and (**b**), Phe409

The chemical shift perturbations induced by formation of the subcomplexes (Δ_{av}) are calculated as $\Delta_{av} = \{[(\Delta\delta_H)^2 + (\Delta\delta_N/5)^2]/2\}^{1/2}$, where $\Delta\delta_H$ and $\Delta\delta_N$ are the chemical shift changes for ^{1}H and ^{15}N, respectively (Grzesiek et al. 1996). They are summarized as a function of the residue number in Fig. 5a and b. The residues with $\Delta_{av} > 0.05$ ppm are mapped on the crystal structure of the β subunit from the $\alpha_3\beta_3$ hexamer (PDB: 1SKY) for the dimer and hexamer in Fig. 5c and d, respectively. The perturbed residues are supposed to interact with the neighboring α subunit or to be affected indirectly by the interaction. The results indicate that the perturbations are larger in the N-terminal domain than those in the C-terminal one, and that the interaction between α and β is weaker in the dimer than in the hexamer.

Discussion

NMR measurement of large molecular systems

TROSY is known to be powerful for large proteins of around 50 kDa. However, CRINEPT worked better for significantly large and complicated protein systems such as F_1 subcomplexes. Since TROSY relies on the magnetization transfer by the INEPT mechanism, its intensity decays close to null with increase of the rotational correlation time (τ_c) (Riek et al. 1999). The exchange among the monomer, dimer, and hexamer may partially contribute to the line-broadening. They would contribute to the lower efficiency of TROSY. Although Wüthrich and his colleagues succeeded in measurement of a 900 kDa complex by means of CRIPT (Fiaux et al. 2002), it was not as efficient as expected in this case. CRIPT is driven by the cross-correlation magnetization transfer and gives splittings not only in the ^{1}H dimension but also in the ^{15}N dimension with alternative phases for proteins with small τ_c (Riek et al. 1999, 2002). The optimum intensity of the sharpest peak scarcely depends on τ_c, supporting applications to much larger molecular systems. Because of partial flexibility of the β subunit, the positive and negative components may remain even in the hexamer, canceling each other out. Although more optimization in experimental conditions such as t_1 might be possible, CRIPT seems to work better for more rigid protein complexes. Consequently, CRINEPT-HMQC-TROSY was found to be the most proper method for investigating a complicated exchange system such as F_1 subcomplexes. CRINEPT intensity is larger than CRIPT one for the proteins with small τ_c and is similar to CRIPT one for those with large τ_c. The simple and symmetric pulse sequence contributes to the better efficiency (Riek et al. 1999, 2002). Furthermore, CRINEPT-HMQC-TROSY can pick up signals not only from rigid parts but also from flexible parts.

Considering the effect of deuteration, the build-up of antiphase coherence on CRIPT and CRINEPT during the magnetization transfer period, T, can be described as follows (Riek et al. 1999).

$$\langle 2I_xS_z\rangle(T) = sinh(R_cT)exp(-R_IT)\langle I_x\rangle(0) \quad (1)$$

with

$$R_I = \frac{2}{5}\left[\frac{2}{9}(\gamma_I B_0 \Delta\sigma_I)^2 + \frac{1}{2}\left(\hbar\gamma_I\gamma_S/r_{IS}^3\right)^2\right]\tau_C + \frac{1}{2T_{1S}} + \frac{1}{2T_{2I}} \quad (2)$$

$$R_c = \frac{4}{15}(\gamma_I B_0 \Delta\sigma_I)\left(\hbar\gamma_I\gamma_S/r_{IS}^3\right)\tau_c \quad (3)$$

where I and S are the ^{1}H and ^{15}N nuclei, and γ, B_0, $\Delta\sigma$, r, and τ_c are the gyromagetic ratio, static magnetic field, chemical shift anisotropy, NH bond length and correlation time, respectively. As discussed in detail previously (Riek et al. 1999, 2002), the efficiency of CRIPT/CRINEPT magnetization transfer is determined by the transverse relaxation rate of ^{1}H, $1/T_{2H}$ in Eq. 2 with $1/T_{2H} >> 1/T_{1N}$ for a large molecule. Signal-width increases with the relaxation contributed by not only amide protons but also

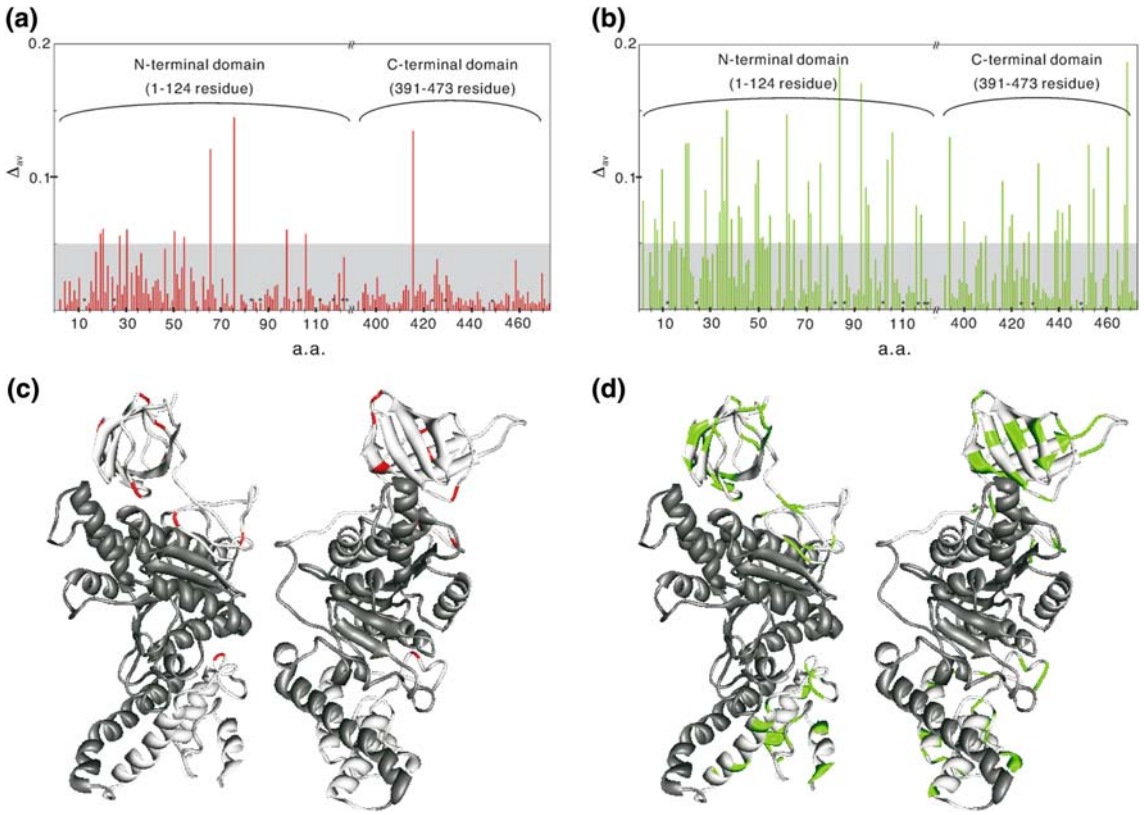

Fig. 5 Chemical shift perturbations (Δ_{av}) as a function of the residue number (**a** and **b**), and mapped on the β structures (**c** and **d**). Red and green stand for the perturbations in heterodimers and hexamers, respectively. (**a** and **b**), no line means not-detected, and the asterisk indicates proline residue. (**c** and **d**), residues with $\Delta_{av} > 0.05$ are mapped on the β subunit (PDB: 1SKY). Left, a side view from the catalytic side; and right, rotated around the vertical axis by 90 degrees and from the putative γ subunit side. These models were drawn using UCSF Chimera (Pettersen et al. 2004)

remote ones. Thus, deuteration is necessary to obtain a high quality spectrum. When both the α and β subunits were not deuterated, the spectral resolution and the S/N ratio at $\alpha/\beta = 1$ were extremely poor (Fig. 2a). With deuteration of the β subunit, the spectrum was significantly improved (Fig. 2b). This is reasonable because the protons in the β subunit are directly involved in the relaxation of NH pairs. Moreover, it was further improved with deuteration of both subunits (Fig. 2c). It can be concluded that even the protons of the α subunit are involved in the relaxation of ^{15}NH spin pairs in the β subunit through strong inter-subunit interactions. There are two possible mechanisms for protons in α to be involved in the NH transverse relaxation in β. One is the direct involvement through the interface. The other is the spin-lattice relaxation time contributing to the line-width (Slichter 1990). The contribution of the latter is usually negligible. Because of slow tumbling of a large molecular system, whole proton spins would form a common reservoir. Here, T_1 would be dominated by the flexible hot spots, becoming short. Under high deuteration, the short T_1 may become detectable.

In spite of the great improvement in its quality, the spectrum in Fig. 2c still suffers from the congestion due to too many signals. This was overcome by segmental isotope-labeling in this work (Fig. 3). Segmental labeling enabled us to get well-resolved information from a large subunit in a huge complex, which is the essential difference from the systems so far reported (Riek et al. 1999, 2002; Fiaux et al. 2002). This work has revealed that the combination of CRINEPT-HMQC-TROSY, deuteration of the whole system, and segmental labeling is the most promising method for analysis of the F_1 complexes, which is our final target.

Dynamic inter-subunit interactions in F_1 subcomplexes

As indicated above, the spectral change was observed for both α/β^*(1–124) and α/β^*(391–473). It was larger for the former than for the latter. This suggests that the N-terminal domain is involved in a stronger inter-subunit interaction. For the heterodimer, there are two possible configurations,

$\alpha\beta$ and $\beta\alpha$, as already described. However, it could not be decided which one is responsible for the observed signals at $\alpha/\beta = 1$ from Fig. 5a and c. The weaker perturbations in both N- and C-terminal domains than those of the hexamer reveal that the dimer structure is not so stable as the hexamer one.

The chemical shift perturbations in the hexmaer are scattered almost all over the labeled region of the N-terminal domain (Fig. 5d). The strong perturbation in the N-terminal domain is reasonable in view of the close contact between the α and β subunits in the TF_1 $\alpha_3\beta_3$ crystal structure (1SKY). This strong interaction might be one of the reasons for in the improvement of the CRINEPT spectrum on deuteration of the α subunit. In contrast, the perturbation in the C-terminal domain (Fig. 5d) was unexpected, because there is scarce contact at the interfaces of the C-terminal domains of the α and β subunits in the crystal structure (Shirakihara et al. 1997). This can be explained only by a movement of the C-terminal domain making contact with the other subunit in the hexamer. Actually, the B factor in the C-terminal domain is larger (100 $Å^2$ in average and 142 $Å^2$ in the DELSEED region) than those in the N-terminal and catalytic domains (47 $Å^2$ and 48 $Å^2$ in average, respectively) even in the crystal structure (Shirakihara et al. 1997). However, the B factor does not manifest whether it comes from structural distribution or motional fluctuation. As indicated in Results, some signals of the C-terminal domain were still doublets even for the hexamer (Fig. 4b). It means that these residues are as mobile as a small molecule even in the 319 kDa hexamer. Most of them fall on the loop regions. These mobile loops may induce a fluctuation of the C-terminal domain. This is completely different from the situation for the loops in the N-terminal domain. Although a well-defined structure is presented for the C-terminal domain in crystal, it is mobile in solution even in the hexamer. Thus, NMR can provide a dynamic view at atomic resolution in contrast to the crystal structure. The hexamer is known to dissociate into dimers on addition of nucleotides (Harada et al. 1991), which induces the conformational change in the β subunit from the open to the closed form and destabilizes the hexamer. Therefore, the motion in the C-terminal domains in solution should be different from that between the open and closed forms. However, the dynamic structure of the C-terminal domain would be important to form a functional structure on the introduction of the γ subunit. Here, a soft interaction between the β and γ subunits generates the catalytic rotation of the γ subunit. The dynamic nature of the C-terminal domain would make it possible. These results suggest that structural heterogeneity is an important feature of such complicated supramolecular complexes as F_1-ATPase. The NMR method developed in this work will contribute to elucidate the mechanism underlying the rotational catalysis of F_1-ATPase.

Acknowledgements This work was partly supported by Grants-in-Aid for Scientific Research on Priority Areas from the Ministry of Education, Science, Technology, Sport and Culture of Japan (HA), and ERATO (MY). We are also grateful to Prof. Takahisa Ikegami (Institute for Protein Research, Osaka University) for his help in the NMR measurements.

References

Abrahams JP, Leslie AGW, Lutter R, Walker JE (1994) Structure at 2.8 Å resolution of F_1-ATPase from bovine heart mitochondria. Nature 370:621–628

Boyer PD (1993) The binding change for ATP synthase—Some probabilities and possibilities. Biochim Biophys Acta 1140: 215–250

Boyer PD (1997) The ATP synthase—a splendid molecular machine. Annu Rev Biochim 66:717–749

Brüschweiler R, Ernst RR (1992) Molecular dynamics monitored by cross-correlated cross relaxation of spins quantized along orthogonal axes. J Chem Phys 96(3):1758–1766

Capaldi RA, Aggeler R (2002) Mechanism of the F_1F_0-type ATP synthase. A biological rotary motor. Trends Biochem Sci 27:154–160

Delaglio F, Grzesiek S, Vuister GW, Zhu G, Pferifer J, Bax A (1995) NMRPipe: a multidimensional spectral processing system based on UNIX pipes. J Biomol NMR 6:277–293

Fernández C, Wider G (2003) TROSY in NMR studies of the structure and function of large biological macromolecules. Curr Opin Struct Biol 13:570–580

Fiaux J, Bertelsen EB, Horwich AL, Wüthrich K (2002) NMR analysis of a 900K GroEL–GroES complex. Nature 418:207–211

Goddard TD and Kneller DG SPARKY3 (2006) University of California, San Francisco. http://www.cgl.ucsf.edu/home/sparky/

Grzesiek S, Bax A, Clore GM, Gronenborn AM, Hu JS, Kaufman J, Palmer I, Stahl SJ, Wingfield PT (1996) The solution structure of HIV-1 Nef reveals an unexpected fold and permits delineation of the binding surface for the SH3 domain of Hck tyrosine protein kinase. Nature Struct Mol Biol 3:340–345

Harada M, Itoh Y, Sato M, Aono O, Ohta S, Kagawa Y (1991) Small-angle X-ray scattering Studies of MgAT(D)P-induced hexamer to dimer dissociation in the reconstituted $\alpha_3\beta_3$ complex of ATP synthase from thermophilic bacterium PS3. J Biol Chem 266:11455–11460

Kagawa Y, Ohta S, Otawara-Hamamoto Y (1989) $\alpha_3\beta_3$ complex of thermophilic ATP synthase catalysis without the γ-subunit. FEBS Lett 249(1):67–69

Mittermaier A, Kay LE (2006) New tools provide new insights in NMR studies of protein dynamics. Science 312:224–228

Miwa K, Yoshida M (1989) The $\alpha_3\beta_3$ complex. the catalytic core of F1-ATPase. Proc Natl Acad Sci 86:6484–6487

Noji H, Yasuda R, Yoshida M, Kinosita K Jr (1997) Direct observation of the rotation of F_1-ATPase. Nature 386:299–302

Ohta S, Yoshida M, Ishizuka M, Hirata H, Hamamoto T, Otawara-Hamamoto Y, Matsuda K, Kagawa Y (1988) Sequence and over-expression of subunits of adenosine triphosphatase in thermophilic bacterium PS3. Biochim Biophys Acta 933: 141–155

Pettersen EF, Goddard TD, Huang CC, Couch GS, Greenblatt DM, Meng EC, Ferrin TE (2004) UCSF chimera—a visualization system for exploratory research and analysis. J Comput Chem 25(13):1605–1612

Riek R, Wider G, Pervushin K, Wüthrich K (1999) Polarization transfer by cross-correlated relaxation in solution NMR with very large molecules. Proc Natl Acad Sci USA 96:4918–4923

Riek R, Fiaux J, Bertelsen EB, Horwich AL, Wüthrich K (2002) Solution NMR techniques for large molecular and supramolecular structures. J Am Chem Soc 124:12144–12153

Saika K, Yoshida M (1995) A minimum catalytic unit of F_1-ATPase shows non-cooperative ATPase activity inherent in a single catalytic site with a K_m 70 μM. FEBS Lett 368:207–210

Shirakihara Y, Leslie AGW, Abrahams JP, Walker JE, Ueda T, Sekimoto Y, Kambara M, Saika K, Kagawa Y, Yoshida M (1997) The crystal structure of the nucleotide-free $\alpha_3\beta_3$ oligomer of F_1-ATPase from the thermophilic Bacillus PS3 is a symmetric trimer. Structure 5:825–836

Slichter CP (1990) Principles of magnetic resonance, 3 edn. Springer-Verlag, New York

Sprangers R, Kay LE (2007) Quantitative dynamics and binding studies of the 20 S proteosome by NMR. Nature 445:618–622

Tozawa K, Yagi H, Hisamatsu K, Ozawa K, Yoshida M, Akutsu H (2001) Functions and ATP-binding responses of the twelve histidine residues in the TF_1-ATPase β subunit. J Biochem 130:527–533

Tugarinov V, Hwang PM, Kay LE (2004) Nuclear magnetic resonance spectroscopy of high-molecular-weight proteins. Annu Rev Biochem 73:107–146

Yagi H, Tozawa K, Sekino N, Iwabuchi T, Yoshida M, Akutsu H (1999) Functional conformation changes in the TF_1-ATPase β subunit probed by 12 tyrosine residues. Biophys J 77:2175–2183

Yagi H, Tsujimoto T, Yamazaki T, Akutsu H (2004) Conformational change of H^+-ATPase β monomer revealed on segmental isotope labeling NMR spectroscopy. J Am Chem Soc 126:16632–16638

Yang D, Kay LE (1999) TROSY triple-resonance four-dimensional NMR spectroscopy of a 46 ns tumbling protein. J Am Chem Soc 121:2571–2575

Yoshida M, Sone N, Arata H, Kagawa Y (1975) A highly stable adenosine triphosphatase from a thermophilc bacterium. J Biol Chem 250:7910–7916

Yoshida M, Sone N, Arata H, Kagawa Y (1977) Reconstitution of adenosine triphosphatase of thermophilic bacterium from purified individual subunits. J Biol Chem 252:3480–3485